JOURNAL OF BACTERIOLOGY, Dec. 2007, p. 8737–8740 Vol. 189, No. 23
0021-9193/07/$08.00+0 doi:10.1128/JB.00899-07

NOTES

Polymerization of the Actin-Like Protein MamK, Which Is Associated with Magnetosomes[▽]

Azuma Taoka,[1]† Ryuji Asada,[1]† Long-Fei Wu,[2] and Yoshihiro Fukumori[1]*

Department of Life Science, Graduate School of Natural Science and Technology, Kanazawa University, Kakuma-machi, Kanazawa 920-1192, Japan,[1] and Laboratoire de Chimie Bactérienne, UPR9043, IBSM, CNRS, 31, Chemin Joseph Aiguier, 13402 Marseille cedex 20, France[2]

Received 8 June 2007/Accepted 20 September 2007

The recombinant actin-like protein MamK was purified from *Escherichia coli* and used as an antigen to generate the anti-MamK antibody. Immunostaining studies showed a linear distribution of MamK in *Magnetospirillum magnetotacticum* cells and of MamK in association with magnetosomes. Moreover, we demonstrated that MamK polymerizes into filamentous bundles in vitro.

Magnetic bacteria synthesize a unique prokaryotic organelle called the magnetosome with which the organisms navigate along the geomagnetic field (1). Magnetosomes consist of membrane-enclosed magnetite crystal particles that are assembled into a straight chain with some structures, such as a magnetosomal matrix, and an interparticle connection (1, 6, 18). The magnetosome chain is positioned at the center of the cell, along the long axis of the cell in the *Magnetospirillum* species. A number of genes encoding magnetosome-associated proteins were identified within the unstable genetic island, referred to as the magnetosome island, in the genomes of the *Magnetospirillum* species and the *Magnetococcus* sp. MC-1 strain (16). This magnetosome island is essential for magnetosome formation and contains at least three operons (*mamAB*, *mamDC*, and *mms*) (15). MamK, which is encoded by the *mamAB* operon, is a new member of the bacterial actin homologue (3, 6, 7, 12, 17). Recently, networks of the cytoskeleton-like filamentous structures were observed along the magnetosome chains of *Magnetospirillum gryphiswaldense*, *M. magneticum* AMB-1, and *M. magnetotacticum* (6, 7, 9, 14). Komeili et al. demonstrated that the Δ*mamK* strain of *M. magneticum* AMB-1 abolishes the filamentous structure near the magnetosomes; hence, the filamentous structure may be composed of MamK (7). Furthermore, we reported that the green fluorescent protein-fused *M. magneticum* AMB-1 MamK protein forms a filamentous organization in the cells of *Escherichia coli* (12). To understand the structure and function of the MamK cytoskeletal filament as well as other bacterial actin homologues, such as MreB and ParM, preparation of the MamK filament in vitro and characterization of the features are required. However, there have been no reports about polymerization of MamK in vitro.

In this study, first, we cloned, expressed, and purified *M. magnetotacticum* MamK from *E. coli*. Second, the localizations of MamK in the wild-type *M. magnetotacticum* cell and in the purified magnetosome chain were confirmed, using immunochemical techniques. Finally, we demonstrated for the first time that the recombinant MamK proteins polymerized into filamentous bundles in vitro.

Localizations of MamK in the *M. magnetotacticum* cell and in the purified magnetosomes. The intracellular localization of MamK was examined and compared to that of MreB by using immunofluorescence microscopy (IFM) with the wild-type *M. magnetotacticum* cell. *M. magnetotacticum* MS-1 (ATCC 31632) was cultured in a chemically defined liquid medium (2) under microaerobic condition at 25°C in the dark and then harvested at the early stationary phase. The C-terminal His-tagged recombinant *M. magnetotacticum* MamK and MreB were overexpressed and purified from *E. coli* C41(DE3) (10) as follows. For construction of the expression plasmids, both genes were amplified by genomic PCR and cloned into pET-29b (Novagen). The primers containing the restriction sites for NdeI (shown underlined) and KpnI (shown with double underlines), mamK-F (5′-GGAATTCCATATGAGTGAAGGT GAAGGCC-3′) and mamK-R (5′-GGGGTACCCGAGCCG GAGACGTCTCCAAGC-3′), were used for the *mamK* cloning, while the primers mreB-F (5′-GGAATTCCATATGTTT TCGAAACTGACGGG-3′) and mreB-R (5′-GGGGTACCG TACATGCTGGTCAGCACGTTC-3′) were used for the *mreB* cloning. The annotated sequences of both MamK (accession no. ZP_00054405) and MreB (accession no. ZP_00055538) in the database lacked the N-terminal residues compared to that of their counterparts from *M. magneticum* AMB-1. Therefore, to express the full-length proteins, DNA sequences encoding the N-terminal 25 amino acids of MamK and the N-terminal 8 amino acids of MreB were added. *E. coli* C41(DE3) cells were transformed and grown at 30°C in LB medium (13) containing 20 μg/ml kanamycin until an optical

* Corresponding author. Mailing address: Department of Life Science, Graduate School of Natural Science and Technology, Kanazawa University, Kakuma-machi, Kanazawa 920-1192, Japan. Phone: 81-76-264-6231. Fax: 81-76-264-6230. E-mail: fukumor@kenroku.kanazawa-u.ac.jp.
† A.T. and R.A. contributed equally to this work.
▽ Published ahead of print on 28 September 2007.

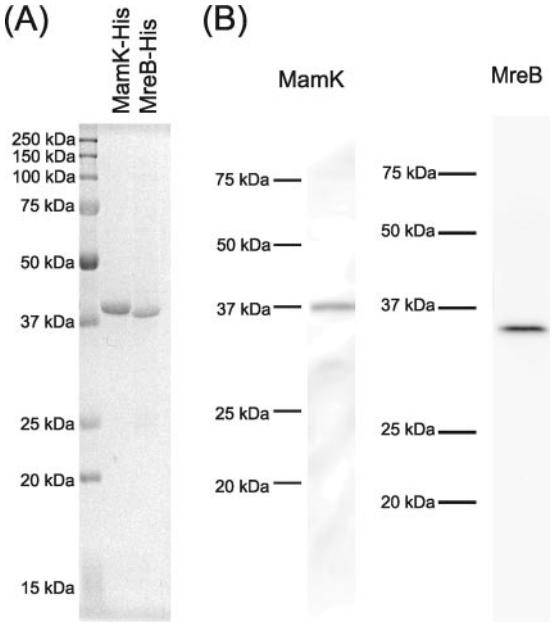

FIG. 1. (A) Sodium dodecyl sulfate-polyacrylamide gel electrophoresis profile of the purified C-terminal His-tagged MamK and MreB from *E. coli* C41(DE3). The protein bands were stained with Coomassie brilliant blue G-250. (B) Immunoblotting analyses of *M. magnetotacticum* cell extract with the anti-MamK and the anti-MreB antibodies. The antibodies generated against MamK and MreB showed monospecificities as single positive bands with apparent molecular masses of 38 kDa and 36 kDa, respectively. The apparent molecular masses of the positive bands corresponded to the deduced molecular masses from the *mamK* and *mreB* genes. Proteins (10 μg/lane) extracted from *M. magnetotacticum* cells were loaded on each lane. The molecular masses of the standards (Precision Plus protein standards; Bio-Rad) are indicated on the left sides of the lanes.

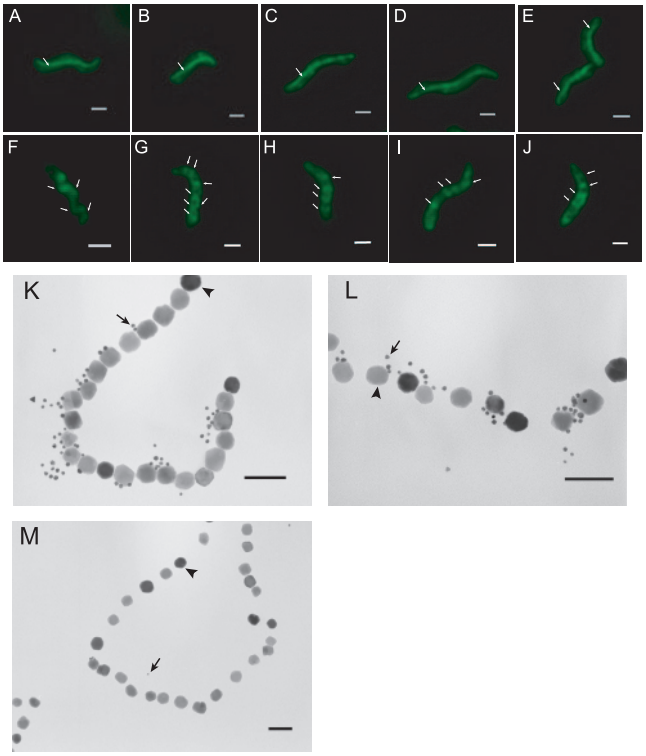

FIG. 2. Localization of MamK in *M. magnetotacticum* cells and in the purified magnetosomes. (A to E) IFM images using the anti-MamK antibody show that MamK formed a linear filamentous structure from pole to pole along the long axis of the *M. magnetotacticum* cells. Arrows show the linear distribution of MamK. (F to J) IFM images using the anti-MreB antibody showing that MreB formed helical filamentous structures in the *M. magnetotacticum* cells. Arrows show the helical localizations of MreB. (K and L) Immunoelectron microscopy images of the purified magnetosomes using the anti-MamK antibody show that the 5-nm gold particles are distributed along the surfaces of the magnetite particles in the magnetosome chains. Arrows and arrowheads show 5-nm gold particles and magnetosomes, respectively. (M) Immunoelectron microscopy image as a negative control experiment using serum prepared from a rabbit prior to immunization showed that only a few gold particles were observed on the magnetosomes. Panel A to J scale bars, 1 μm; panel K to M scale bars, 100 nm.

density at 600 nm of 0.6 was reached, and then the recombinant proteins were induced with 0.1 mM isopropyl-β-D-thiogalactopyranoside for 5 h. Both recombinant proteins were purified from inclusion bodies for the generation of antigens, using Ni^{2+} affinity chromatography (Ni-nitrilotriacetic acid agarose; Qiagen) under denaturing conditions, according to the Qiagen technical manual (Fig. 1A). The anti-MamK and anti-MreB polyclonal rabbit antibodies were raised against the purified His-tagged MamK and MreB proteins, respectively. Also, the cell extract of *M. magnetotacticum* was separated by sodium dodecyl sulfate-polyacrylamide gel electrophoresis (8) and then used for immunoblotting (18) or quantitative immunoblotting (11), as described previously. The immunoblotting analyses using both antibodies showed that each single positive band corresponded to the molecular mass deduced from the *mamK* and *mreB* genes and also showed no cross-reactivities (Fig. 1B). Furthermore, the quantitative immunoblotting analyses estimated that the cellular amounts were 26,000 ± 6,000 ($n = 8$) MamK molecules per cell and 5,000 ± 1,000 ($n = 6$) MreB molecules per cell. Because the longitudinal monomer spacing of other actin-like proteins, such as MreB and ParM, approximately 51 Å and 49 Å, respectively (19, 20), the *M. magnetotacticum* cell seems to contain enough MamK molecules to exist as a bundle of protofilaments or as a network structure along the long axis of the cell.

IFM was performed as previously described (5), with slight modifications. The anti-MamK and anti-MreB antisera were used at a 1:100 dilution, and the secondary fluorescein isothiocyanate-conjugated anti-rabbit immunoglobulin G (EY Laboratories) was used at a 1:1,500 dilution. IFM demonstrated that MamK was distributed in a line from pole to pole along the long axis of the *M. magnetotacticum* cells (Fig. 2A to E). This is the first observation of the MamK localization in the cell of *M. magnetotacticum*. The MamK distribution in the *M. magnetotacticum* cell was consistent with that of *M. magneticum* AMB-1 as reported in previous studies (7, 12). Whereas, MreB showed a spiral distribution in *M. magnetotacticum* cells (Fig. 2F to J), these results proved that two kinds of actin-like proteins were assembled into different organizations in the *M. magnetotacticum* cell.

Furthermore, immunoelectron microscopy of the purified magnetosomes, using the anti-MamK antibody, which was performed using a JEOL JEM 2000EX transmission electron mi-

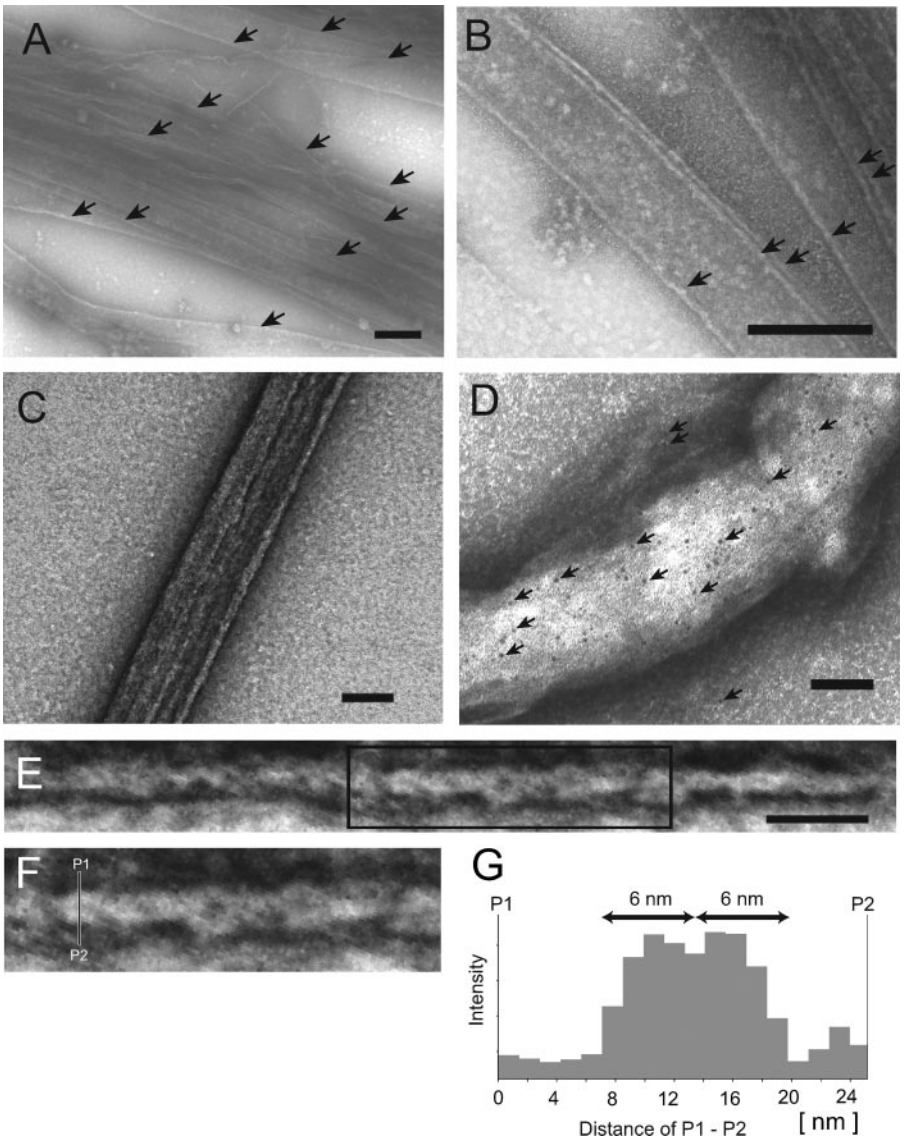

FIG. 3. TEM images of negatively stained MamK polymers. (A and B) Filamentous bundles of MamK. Arrows show the synthesized filamentous bundles of MamK. (C) The well-developed bundle of MamK. (D) Immunogold staining of the synthesized bundle using anti-MamK antibody. The arrows show the 5-nm gold particles. Many gold particles are attached to the bundle; in contrast, few gold particles are attached to the background. (E) The filamentous bundle ranged from 8 to 18 nm in width. (F) An enlargement of the box from panel E is shown. Each bundle consisted of fine helical filaments. (G) A line profile P1 to P2 of intensity from the enlarged bundle shown in panel F. Double-head arrows show the width of a single helical filament. The helical filament was about 6 nm in width. Panel A to C scale bars, 200 nm; panel D scale bar, 100 nm; panel E scale bar, 50 nm.

croscope (TEM) as previously described (18), showed that the gold particles were distributed along the surfaces of the magnetite particles in the magnetosomes (Fig. 2K and L). This result suggested that MamK is localized in the structure of the magnetosome chain, whereas only a few gold particles were observed in the negative control experiment using the serum prepared from the rabbit prior to immunization (Fig. 2M).

Polymerization of MamK in vitro. The polymerization of MamK was examined using electron microscopy. Soluble His-tagged MamK was purified from the soluble fraction of *E. coli* for the MamK polymerization experiment. The *E. coli* cells were disrupted with sonication, and then the lysate was centrifuged at 100,000 × *g* for 1 h. The supernatant was subjected to Ni^{2+} affinity chromatography (Ni-nitrilotriacetic acid agarose; Qiagen) under native conditions, according to the Qiagen technical manual. The purified MamK was added at a final concentration of 10 μM in a total volume of 30 μl of polymerization buffer containing 100 mM Tris-HCl (pH 7.0), 14 mM $MgCl_2$, 100 mM NaCl, and 30 mM KCl. The mixture was then centrifuged at 150,000 × *g* for 1 h to remove the aggregates. After the addition of 2 mM (final concentration) ATP or the nonhydrolyzable ATP analogue adenosine-5′-(γ-thio)triphosphate (ATP-γ-S), the mixture was incubated at 30°C for 5 min. Formvar- and carbon-coated grids were put on a drop of the resulting mixture for 5 min. The grids were washed twice on a drop of water for 2 min each time and then were negatively

stained with 4% uranyl acetate. The products on the grids were observed using a JEOL JEM 2000EX transmission electron microscope (TEM) or a JEOL JEM-2010FEF TEM equipped with an Advanced Scanning Imaging Device unit. Before the MamK polymerization experiment, we used TEM to confirm that there is no filamentous structure in the purified MamK sample. In the case of the ATP addition, we could not observe any filamentous structures on the grids. On the other hand, we found that MamK was polymerized into long straight filamentous bundles by adding ATP-γ-S instead of ATP (Fig. 3A and B). These results suggest that although the polymerized MamK prepared by the addition of ATP-γ-S is stable, the MamK filaments with ATP might be depolymerized during the preparation procedure. The well-developed bundles were more than 100 μm in length and 100 nm in width (Fig. 3C). Immunogold staining of the bundles with the anti-MamK antibody confirmed that the bundles were composed of MamK proteins (Fig. 3D). The smallest bundles were twisted, with total diameters of 8 to 18 nm (Fig. 3E). Furthermore, the twisted bundles were composed of fine helical filaments, which were about 6 nm in width (Fig. 3F and G). The fine helical filaments seemed to be protofilaments.

The actin-like protein ParM polymer forms a gently twisted double-helical filament, and the ParM filament is unlikely to be bundled (19). The MreB polymer, which is observed as a straight or curved protofilament, is arranged in a filamentous bundle or a ring-like structure (4, 20). In contrast, the polymerized MamK appears as straight, long, filamentous bundles, and the smallest MamK bundle consisted of fine helical filaments. Accordingly, the nature of MamK polymer is distinct from the other known actin-like proteins. Although these specific features of the polymerized MamK might contribute to the magnetosomes' formation and magnetoreception, additional research is required to determine the structure and characteristics of the MamK cytoskeletal filament. The magnetosome chain consists of some additional structures, e.g., a membrane vesicle, a cytoskeletal filament, and a magnetosomal matrix. These components are highly ordered with various magnetosome-associated proteins. The reconstruction of the magnetosomal components in vitro would provide new insights into the elucidation of the functions of magnetosome-associated proteins and the mechanism of magnetosome formation. The present study provides the first step for the in vitro reconstruction studies of the magnetosomal structures.

This work was supported by a Human Frontier Science Program Research Grant (RGP0035/2004-C104) to Y.F. and a Grant-in-Aid for Scientific Research on Priority Areas (no. 16087205) to Y.F. from the Ministry of Education, Culture, Sports, Science and Technology of Japan.

We thank K. Tazaki (Kanazawa Univ.) for the TEM, Y. Sasayama (Kanazawa Univ.) for the fluorescence microscope facilities, and M. Kanemori (Kanazawa Univ.) for helpful discussion.

REFERENCES

1. **Bazylinski, D. A., and R. B. Frankel.** 2004. Magnetosome formation in prokaryotes. Nat. Rev. Microbiol. **2:**217–230.
2. **Blakemore, R. P., D. Maratea, and R. S. Wolfe.** 1979. Isolation and pure culture of a freshwater magnetic spirillum in chemically defined medium. J. Bacteriol. **140:**720–729.
3. **Carballido-López, R.** 2006. The bacterial actin-like cytoskeleton. Microbiol. Mol. Biol. Rev. **70:**888–909.
4. **Esue, O., M. Cordero, D. Wirtz, and Y. Tseng.** 2005. The assembly of MreB, a prokaryotic homolog of actin. J. Biol. Chem. **280:**2628–2635.
5. **Figge, R. M., A. V. Divakaruni, and J. W. Gober.** 2004. MreB, the cell shape-determining bacterial actin homologue, co-ordinates cell wall morphogenesis in *Caulobacter crescentus*. Mol. Microbiol. **51:**1321–1332.
6. **Komeili, A.** 2007. Molecular mechanisms of magnetosome formation. Annu. Rev. Biochem. **76:**351–366.
7. **Komeili, A., Z. Li, D. K. Newman, and G. J. Jensen.** 2006. Magnetosomes are cell membrane invaginations organized by the actin-like protein MamK. Science **311:**242–245.
8. **Laemmli, U. K.** 1970. Cleavage of structural proteins during the assembly of the head of bacteriophage T4. Nature **227:**680–685.
9. **Martins, J. L., C. N. Keim, M. Farina, B. Kachar, and U. Lins.** 2007. Deep-etching electron microscopy of cells of *Magnetospirillum magnetotacticum*: evidence for filamentous structures connecting the magnetosome chain to the cell surface. Curr. Microbiol. **54:**1–4.
10. **Miroux, B., and J. E. Walker.** 1996. Over-production of proteins in *Escherichia coli*: mutant hosts that allow synthesis of some membrane proteins and globular proteins at high levels. J. Mol. Biol. **260:**289–298.
11. **Møller-Jensen, J., R. B. Jensen, J. Löwe, and K. Gerdes.** 2002. Prokaryotic DNA segregation by an actin-like filament. EMBO J. **21:**3119–3127.
12. **Pradel, N., C.-L. Santini, A. Bernadac, Y. Fukumori, and L.-F. Wu.** 2006. Biogenesis of actin-like bacterial cytoskeletal filaments destined for positioning prokaryotic magnetic organelles. Proc. Natl. Acad. Sci. USA **103:**17485–17489.
13. **Sambrook, J., and D. W. Russell.** 2001. Molecular cloning: a laboratory manual, 3rd ed. Cold Spring Harbor Laboratory Press, Cold Spring Harbor, NY.
14. **Scheffel, A., M. Gruska, D. Faivre, A. Linaroudis, J. M. Plitzko, and D. Schüler.** 2006. An acidic protein aligns magnetosomes along a filamentous structure in magnetotactic bacteria. Nature **440:**110–114.
15. **Schübbe, S., C. Würdemann, J. Peplies, U. Heyen, C. Wawer, F. O. Glöckner, and D. Schüler.** 2006. Transcriptional organization and regulation of magnetosome operons in *Magnetospirillum gryphiswaldense*. Appl. Environ. Microbiol. **72:**5757–5765.
16. **Schüler, D.** 2004. Molecular analysis of a subcellular compartment: the magnetosome membrane in *Magnetospirillum gryphiswaldense*. Arch. Microbiol. **181:**1–7.
17. **Shih, Y.-L., and L. Rothfield.** 2006. The bacterial cytoskeleton. Microbiol. Mol. Biol. Rev. **70:**729–754.
18. **Taoka, A., R. Asada, H. Sasaki, K. Anzawa, L.-F. Wu, and Y. Fukumori.** 2006. Spatial localizations of Mam22 and Mam12 in the magnetosomes of *Magnetospirillum magnetotacticum*. J. Bacteriol. **188:**3805–3812.
19. **van den Ent, F., J. Møller-Jensen, L. A. Amos, K. Gerdes, and J. Löwe.** 2002. F-actin-like filaments formed by plasmid segregation protein ParM. EMBO J. **21:**6935–6943.
20. **van den Ent, F., L. A. Amos, and J. Löwe.** 2001. Prokaryotic origin of the actin cytoskeleton. Nature **413:**39–44.